Simulation of Myelin Water Imaging

Junyu Guo[1] and Wilburn E. Reddick[1]
[1]*Division of Translational Imaging Research, St Jude Children Research Hospital, Memphis, TN, United States*

INTRODUCTION: Myelin water imaging is a promising, noninvasive technique for evaluating white matter diseases using myelin water fraction (MWF) as a direct indicator of myelin component change due to white matter diseases such as multiple sclerosis (MS)[1]. A new method with an efficient acquisition scheme, T_2 spectrum analysis using a weighted regularized non-negative least squares algorithm and non-local mean filter (T_2SPARC), was proposed to achieve a shorter acquisition time, higher image quality, and large volume coverage [2]. In the T_2SPARC method, a large regularization coefficient of $\mu = 1.8$ was empirically selected in the weighted regularized non-negative least squares (wrNNLS) algorithm to balance the sensitivity and reliability to measure MWF values. In this study, simulations were performed to compare wrNNLS with the formerly used regularized non-negative least squares (rNNLS) algorithm and validate this empirically selected μ value.

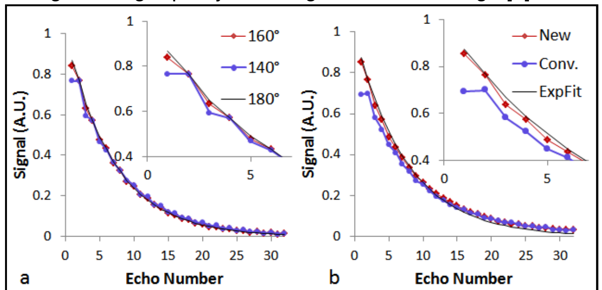

Fig. 1 Comparison between simulated and in vivo decay curves. a) simulation results. (b) in vivo results. ExpFit represents fitting the first ten data points except the first one.

METHOD: The T_2SPARC method utilized a modified multi-slice CPMG sequence with a refocusing slice thickness three times the size of the excitation slice thickness to reduce the effect of imperfect refocusing RF pulses and optimize T_2 decay curves [2]. The extended phase graph (EPG) algorithm was used to simulate the effect of imperfect refocusing RF on the signal decay [3]. The refocusing RF pulses of 140°, 160° and 180° with T_1=1100 ms and T_2=70 ms for white matter were selected to simulate three situations: 1. a conventional CPMG sequence; 2. a new modified CPMG sequence; 3. an ideal sequence. The simulated results were compared with the decay curves from an in vivo study to identify and calculate variations generated by imperfect RF for the third simulations. In the T_2SPARC method, the new wrNNLS algorithm was proposed to overcome the shortcomings of the rNNLS algorithm and generate robust and high-quality MWF maps [2]. The rNNLS algorithm is as follows:

$$\min_{S_T}\{\|ES_T - Y\|_2 + \mu\|S_T\|_2\},\ E_{nm} = e^{-\frac{t_n}{T_{2m}}}, S_T = S_m \Delta T_{2m},\ S_T \geq 0 \qquad (1)$$

The wrNNLS algorithm is as follows:

$$\min_{S_T}\{\|ES_T - Y\|_2 + \mu\|WS_T\|_2\},\ E_{nm} = e^{-\frac{t_n}{T_{2m}}}, W_m = 1/\Delta T_{2m},\ S_T \geq 0 \qquad (2)$$

where S_T is the weighted spectral amplitude, S_m is the spectral amplitude, Y is the decay signal intensity, t_n is the n^{th} echo time, ΔT_{2m} is a logarithmic T_2 interval, and μ is the regularization coefficient. The number of T_2 sampling points of 96 was chosen to balance computation efficiency and spectral accuracy. The effective regularization coefficient of the rNNLS and wrNNLS algorithms using logarithmically spaced sampling are $\mu \cdot \Delta T_{2m}$ and μ, respectively. A simulation was performed to investigate the effect of different T_2 values on the regularization of T_2 spectrum when using two algorithms with a small $\mu = 0.02$. Finally, simulations using different μ values were performed to investigate the optimal μ values for both algorithms in three situations: a. original simulated ideal decaying signal comparable to in vivo results; b. signal with Gaussian noise with a variance of 20 (the signal at the first point is 1230); c. signal with Gaussian noise and variations generated in the first simulation due to imperfect RF. The large variations at the first three points were added into the signal and the variations in the other points with larger TE values were neglected.

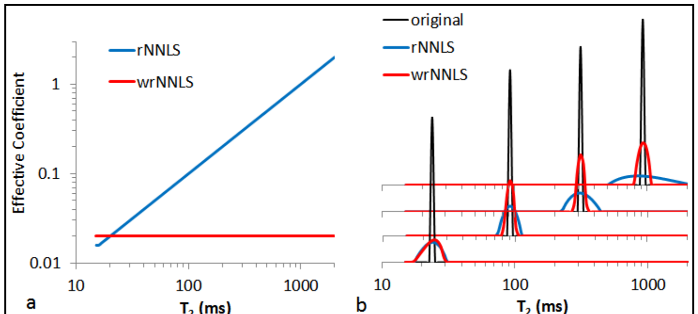

Fig. 2 Comparison of reguarization between rNNLS and wrNNLS. a. Effective regularization coefficient with $\mu = 0.02$. b. Regularized T_2 spectra at four T_2 time points with $\mu = 0.02$.

RESULTS: Fig. 1a shows the simulated decay curves using the EPG for three types of refocusing RF pluses. Fig. 1b shows in vivo decay curves from a healthy volunteer. "New" represents the new modified sequence; "Conv." represents the conventional CPMG sequence. The similar patterns of variation caused by imperfect RF are shown in both figures. The new refocusing RF pulse led to a substantially ameliorated T_2 decay curve. The variations of the first three points using 160° from those using the perfect refocusing pulse 180° in Fig.1a were calculated and applied in the third simulation. Fig.2a shows the effective regularization coefficients for both algorithms with the prescribed $\mu = 0.02$. The effective coefficients of rNNLS increases as T_2 and could be as large as 2 when T_2 is near 2000 ms, which is even larger than the empirical μ value of 1.8 for wrNNLS. This increasing regularization effects of rNNLS as T2 increases are shown in Fig. 2b. Fig. 3 shows calculated MWF values for different μ values using both algorithms in three situations. The true MWF is 11%. The μ values of the crossing points marked by arrows were 0.29, 0.3, and 0.41 for rNNLS, and were 0.99, 1.05, and 1.66 for wrNNLS. Noise was only a small factor of the change of the μ value of the crossing point, and adding variations caused a larger change of the μ value. For wrNNLS, $\mu = 1.66$ is very close to the empirically determined value of 1.8.

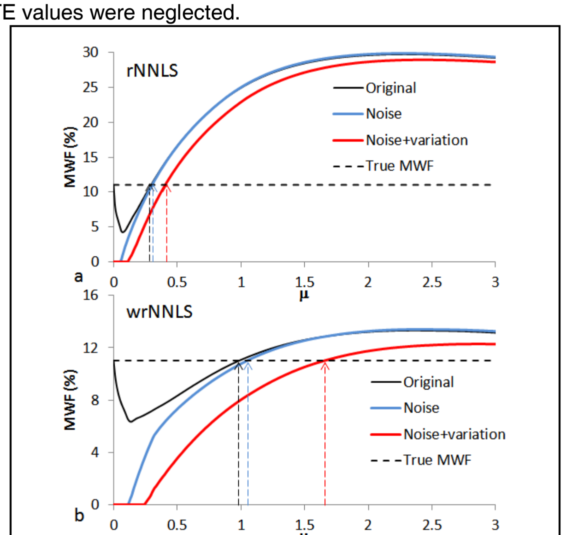

Fig. 3 Comparison of calculated MWFs between rNNLS and wrNNLS for different μ values in three situations. a. Results using rNNLS; b. Results using wrNNLS.

CONCLUSION: We compared the performance of rNNLS and wrNNLS algorithms using simulations. The rNNLS algorithm had a much larger effective regularization for a larger T_2 value and the wrNNLS algorithm had a uniformed effective regularization coefficient when using a logarithmically spaced sampling. The empirically selected μ value of 1.8 for wrNNLS is very close to the optimized value of 1.66 in the simulations.

REFERENCE:

1. Whittall et al. MRM, 1997. 37(1): p. 34-43. 2. Guo et al. MRM, 2012, in press. 3. Hennig J. Concepts in MR, 1991. 3: p125-143